

An Extended Hückel Study of Two Dimensional Layered Compound: FeOCl

Sang-Ho Kim and Hojing Kim*

Department of Chemistry, Seoul National University, Seoul 151-742

Research Institute of Molecular Sciences, Seoul National University, Seoul 151-742

Received September 26, 1992

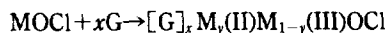
The electronic structure of two dimensional layered compound, FeOCl, is studied with the band model and the cluster model approximation employing Extended-Hückel (EH) method. We examine the effects of intercalation (*e.g.*, localization of transferred electron, conductivity increase). FeOCl has the electronic structure typical for layered compounds as expected. For FeOCl-Li_{1/2} system, the charge transfer from Li to the FeOCl lattice occurs, and electrons are built up almost exclusively on Fe atoms. The partially filled band of FeOCl-Li_{1/2} complex is responsible for the increase in conductivity.

Introduction

Layered compounds have been widely studied on account of their distinguished physical properties arising from the two dimensional nature. There have been many efforts to examine the physical properties and electronic structures of layered materials.¹⁻³ When a layered material can take up reversibly electropositive elements such as Li or Na into its van der Waals gap, it can be used as a cathod material. Transition-metal dichalcogenides, *e.g.*, TiS₂, TaS₂, and MoS₂, are well-known examples investigated for this purpose. FeOCl is also one of the promising cathod materials for the high-energy density secondary battery if it had not the frailty under the humid atmosphere.⁴ Due to the lowest electronegativity, lithium has been considered to be the very good anode material which gives up electrons most easily to form positive ions. Thus studies on the intercalation of unsolvated metal ions in layered materials have focused almost exclusively on Li⁺.

Layered transition-metal oxychlorides (MOCl with M=Ti, V, Cr, Fe, and In) can intercalate various electron donors or Lewis bases such as alkali metals, metallocenes and many organic molecules.⁵⁻⁹ However, there exist remarkable differences with the choice of central metals in electrical conductivity, magnetic behavior, the reactivity of intercalation or substitution, and so on. The five metal oxychlorides have nearly identical structures and ligand fields. The *d*-orbital electrons of central metals are regarded as the major factor affecting the differences.

Intercalation has been accepted as a kind of electron donor-acceptor reaction between host and guest, leaving the host matrix in a partially reduced state. Since the transferred electrons from guest (G) to MOCl are considered to be localized on the central metal, the intercalation of MOCl with the guest molecules can be represented as follows:



where *x* and *y* stand for the amount of intercalated guest and transferred electron, respectively. The equation assumes that there is no band structure in MOCl and thus only the central metal is reduced in the electron transfer reaction.¹⁰ In order to check the validity of the above assertion, we

have calculated the band structure of FeOCl and its lithium intercalation complex using EH approximation. Many informations have been obtained by the cluster model EH-MO calculation. The charge distribution has been estimated by calculating the net charge of each constituting atom.

A quantitative calculation for layered compound was carried out by McCanny (1979) who obtained the band structure of LiTiS₂ using the simple tight-binding method.¹ The self-consistent band structure of LiTiS₂ was studied by Umrigar *et al.* (1982).² LiTaS₂ was calculated by Guo and Liang (1987) using self-consistent LMTO method.³ Up to now, however, no band electronic structure calculation has been reported for this interesting compound. The fact that the intercalation reaction can alter the basic properties of the host MOCl has provided the driving force for a better understanding of the electronic structure with this rather remarkable solid state system. We examine how the electronic structure of FeOCl is related to its physical properties and discuss the mechanism for this intercalation reaction.

Computational Details

To derive the electronic structure of FeOCl, we have carried out two types of calculations: EH-band calculation¹¹⁻¹³ and EH cluster model approximation. Usually, band calculations of layered materials are performed within 2D Brillouin zone. In this study, however, since our interest is focused on the effect of intercalation on the layers, we have solved the Schrödinger equation at several *k*-points within 3D Brillouin zone. For the cluster model approximation, we have chosen (FeOCl)₁₆ cluster. The size of the cluster is a result of the compromise between ease of computation and conservation of solid nature. The unit cell geometry is adopted from the X-ray data of Lind.¹⁴ The FeOCl structure in the present study is conveniently assumed to have the symmetry of the D_{2h}³ (P_{mmm}) space group, which belongs to the orthorhombic system. This model is presented in Figure 1.

The Brillouin zone is a simple orthorhombic, as shown in Figure 2, which also shows the irreducible wedge ZURTT-XSY. The energy band structure was calculated along this symmetry line.

The EH parameters used in this calculation are collected

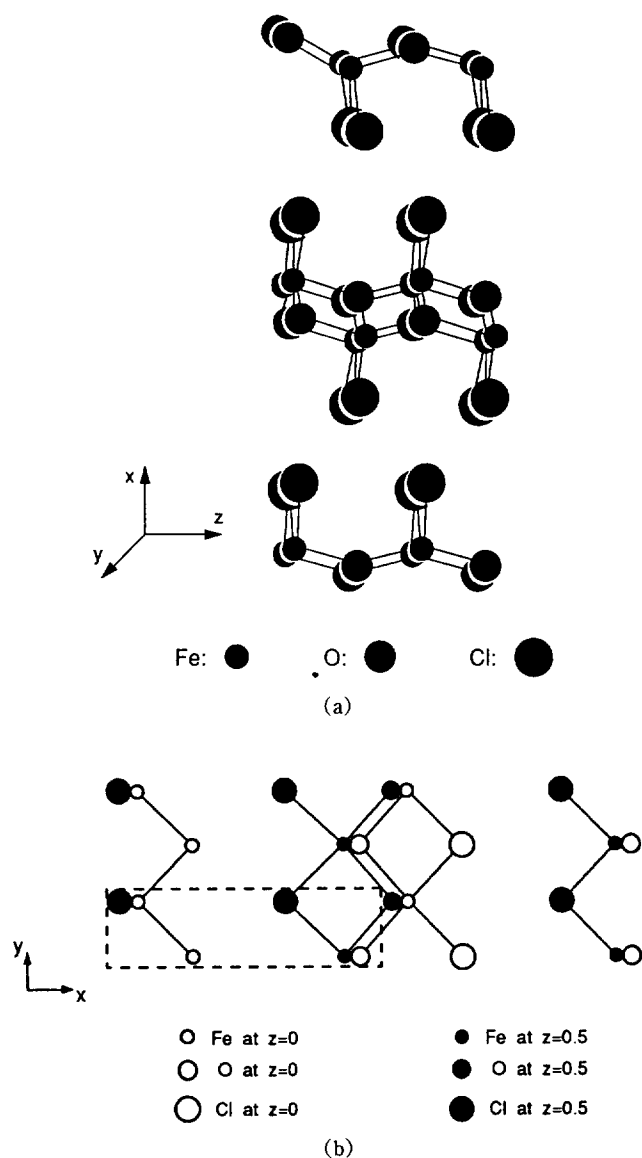


Figure 1. The geometry of $(\text{FeOCl})_{16}$ cluster. (a) Three dimensional structure. (b) Projection on xy plane. The dotted box in (b) represents the unit cell for the band calculation.

Table 1. Extended Hückel Parameters

Orbital	H_{ii}	ζ_1^a	ζ_2^b	C_1^a	C_2^b
Fe 4s	-9.10	1.900			
Fe 4p	-5.32	1.900			
Fe 3d	-12.60	5.350	2.000	0.5505	0.6260
O 2s	-32.30	2.275			
O 2p	-14.80	2.275			
Cl 3s	-30.00	2.033			
Cl 3p	-15.00	2.033			
Cl 3d	-9.00	2.033			
Li 2s	-5.40	0.650			
Li 2p	-3.50	0.650			

^aExponent in a double- ζ expansion of the metal d -orbitals. ^bCoefficients in a double- ζ expansion of the metal d -orbitals.

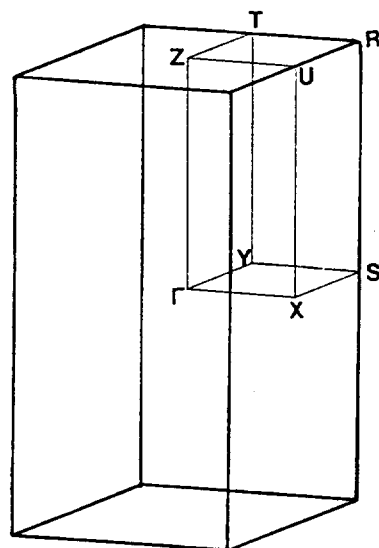


Figure 2. The Brillouin zone for the FeOCl. Γ XSYZURT is the irreducible wedge.

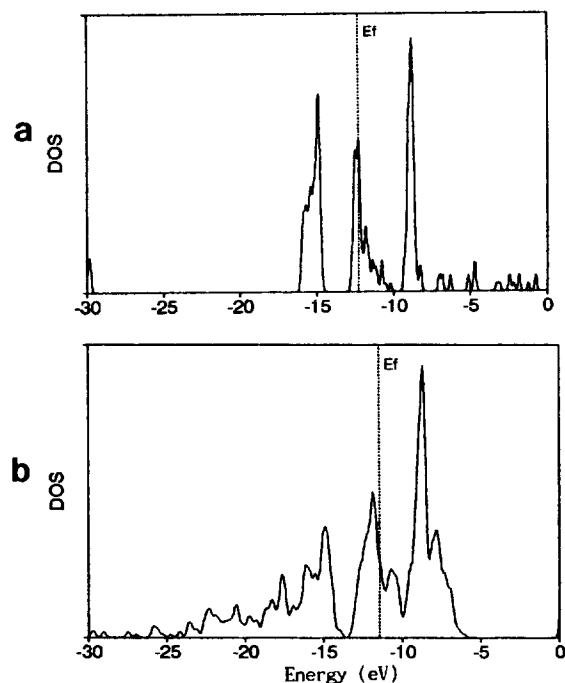


Figure 3. (a) The DOS curve of $(\text{FeOCl})_{16}$ using EH-MO calculation. $E_f = -12.18$ eV. (b) The DOS curve of FeOCl using EH-band calculation. $E_f = -11.61$ eV. The dotted lines indicate the Fermi energy of each calculation. For convenience, the HOMO energy is regarded as Fermi Energy.

in Table 1. The parameters for Fe are taken from the work of Hoffmann on the Fe_2L_6 .¹⁵

The Electronic Structure of Host Material: FeOCl.

In order to follow the development with intercalation, the electronic structure of the host FeOCl is calculated first.

Figure 3 represents the density of states (DOS) curves of FeOCl obtained by EH-MO calculations and EH-band calculations, respectively. These two curves show the resemblance except for the slight difference in the Fermi level. Al-

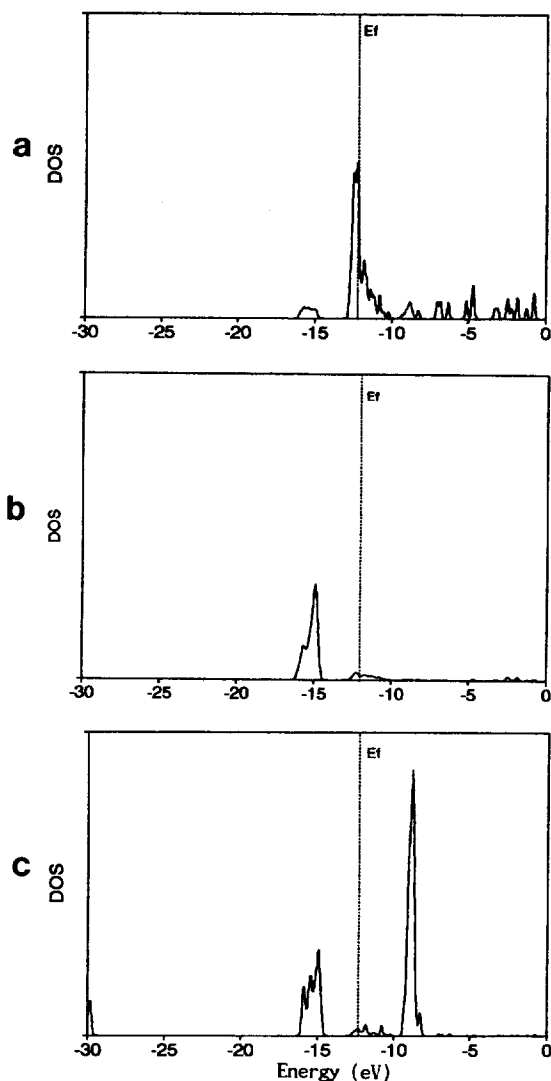


Figure 4. The PDOS curves onto the 3 atoms of FeOCl using EH-MO calculation. (a) Projection on Fe atom. (b) Projection on O atom. (c) Projection on Cl atom. The dotted lines indicate the Fermi energy.

though the DOS curve for the band calculation are broader than that of MO calculation, the peaks indicate qualitatively similar patterns – more interactions between the neighbor cells cause the peak broadening in the band calculation. These DOS curves imply that the two calculations are complementary to each other. That is, the cluster approximation may be applicable to the calculation of material with translational symmetry. Although the band model is more adequate in such system, one can derive less informations than from the cluster model calculation. In fact, calculations for many physical properties using the perturbation theory have been carried out by cluster model approximation.¹⁶ So, it is hopeful that there is a correspondence between these two types of calculations. Thus we may expect to obtain more informations from the combination of EH-MO and EH-band calculation than from the band calculation only.

In Figure 4, we show the projections (PDOS) onto the 3 atoms (Fe, O, Cl) from DOS of EH-MO calculation. The PDOS curves obtained from band calculation are omitted due

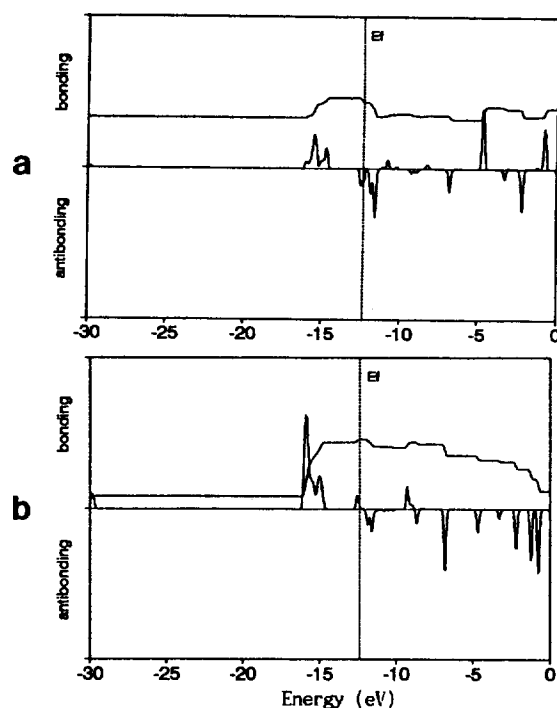


Figure 5. The COOP curves of each bond using EH-MO method. (a) Fe-O bond, (b) Fe-Cl bond, The dotted lines indicate the Fermi energy.

to the similarity of patterns with MO calculation. The PDOS represents the contribution of a certain fragment (orbital or atom) of a system to the total DOS. Comparing DOS of FeOCl with PDOS of its constituting atoms, we can see the contribution near the Fermi level originates almost entirely from the Fe 3d-orbitals. The minor contribution from Cl atom is observed. That is, if the charge transfer occurs due to the intercalation of electron donating compounds (e.g., Li, pyridine and alkyl amines) to the FeOCl lattice, the transferred electrons are built up predominantly in the central Fe atoms.

The crystal orbital overlap population (COOP) curves shown in Figure 5 reflect the bonding nature of orbitals. The COOP of A-B bond is defined as follows:¹⁷

$$\begin{aligned} \text{COOP } dE &= 2\delta(E-E_a) \sum_{i \in A} \sum_{j \in B} C_{ia} C_{ja} S_{ij} dE & (1) \\ &= \frac{2}{(\pi\sigma^2)^{1/2}} \sum_{i \in A} \sum_{j \in B} C_{ia} C_{ja} S_{ij} \\ &\quad \times \exp[-(E-E_a)^2/(2\sigma^2)] dE & (2) \end{aligned}$$

where C_{ia} is the i th coefficient of a th MO and S_{ij} is an overlap integral of i th basis and j th basis. A and B could be atoms or fragments. σ is an arbitrary smoothing parameter in a Gaussian function. In finite system, Eq. (1) can be substituted by Eq. (2). The positive region of the COOP curve corresponds to bonding and the negative to antibonding. Thus we can conclude the molecular orbital (MO) at the Fermi level is weakly bonding between Fe and Cl. Whereas the MO above the Fermi level (which is considered to be occupied when the intercalation occurs) is an antibonding orbital between Fe and O.

In Figure 6, we give the energy band structure of FeOCl

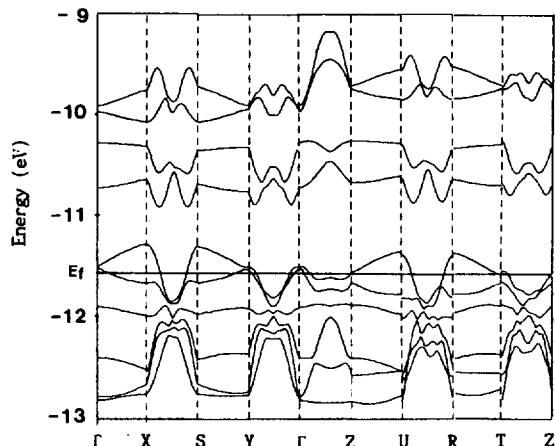


Figure 6. The energy band structure of FeOCl using EH-band calculation. This contains the d bands of Fe in the region -13 – -9 eV.

along certain symmetry lines in the Brillouin zone. This contains the Fe d -bands in the region between -13.0 and -9.0 eV. As seen in Figure 1, the Fe atoms are located in the distorted octahedral sites. So we can refer the low-lying 6 bands to t_{2g} -block bands and upper-lying 4 bands to e_g -block bands. As shown in Figure 6, the Fermi level locates at the upper edge of t_{2g} -block band. For the unit cell $(\text{FeOCl})_2$, there are 10 electrons to fill the 5 t_{2g} -block band. The band gap between the highest occupied band (HO-band) and lowest unoccupied band (LU-band) is *ca.* 0.2 eV, which is inconsistent with the fact that FeOCl is a semiconductor with resistivity, $\rho \sim 10^7 \Omega\text{cm}$. The inconsistency is expected since non-self-consistent calculations tends to overestimate the p - d gap and underestimate band width.³ Nevertheless we may predict the properties of host molecule qualitatively from the shape of each band.

As mentioned earlier, since FeOCl is a layered compound, we can expect that FeOCl gives the characteristic electronic structure of 2D material. When the HO-band does not cross a Fermi surface along a certain wave vector direction, there are no electrons at the Fermi level having momentum along that direction so that the system is not metallic along that direction.¹¹ As shown in Figure 6, the bands are nearly flat along x direction so that only one band crosses the Fermi surface. To the contrary, the bands are dispersive along y and z directions. Thus we can expect that the in-plane conductivity (σ_{\parallel}) is larger than the perpendicular one (σ_{\perp}). Looking the structural features of FeOCl, van der Waals gaps are located on the yz plane so that the orbital interactions between the sheets are very weak. Thus the above expectation is quite natural and consistent with the experimental data.¹⁸

The Li intercalated complex: FeOCl-Li_{1/2}. Now let us consider what changes will be brought out due to the lithiation of FeOCl. In this calculation we use the model proposed by Rouxel.⁴ He calculated the potential energy minimum by regarding Li⁺ ion as point charge. Figure 7, we adopted the position of Li obtained by this method.

In Figure 8, we present the band structure of the FeOCl-Li_{1/2}. Compared with Figure 6, it is clear that the two band structures are substantially similar. The significant changes

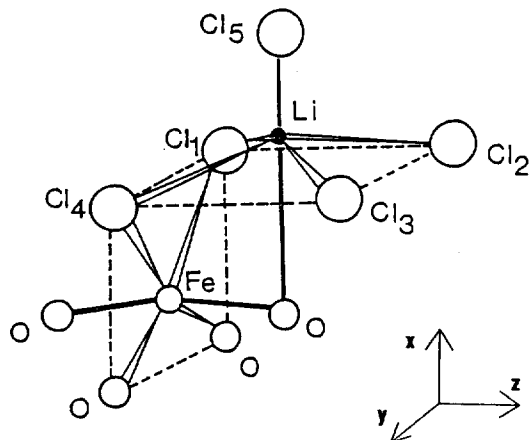


Figure 7. The position of Li atom in FeOCl-Li_{1/2} complex. Li is surrounded by 4 equatorial Cl atoms, 1 axial Cl atom, and 1 axial O atom.

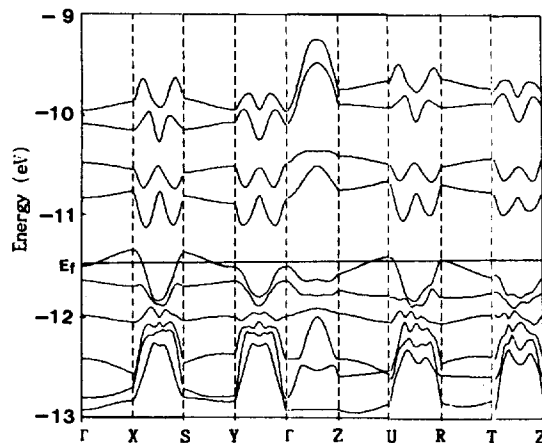


Figure 8. The energy band structure of FeOCl-Li_{1/2} using EH-band calculation. The Fermi energy is -11.58 eV. This contains d band of Fe in the region -13 – -9 eV.

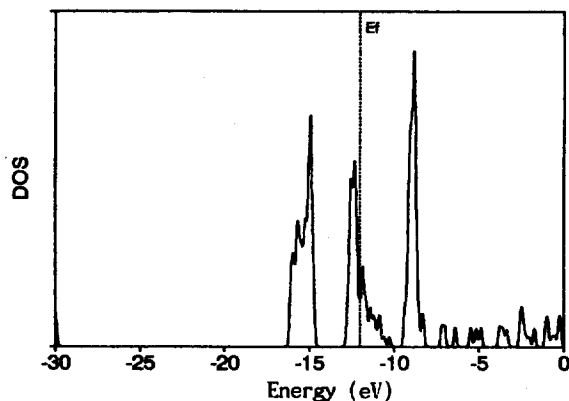


Figure 9. The DOS curve of $(\text{FeOCl-Li}_{1/2})$ using EH-MO calculation. $E_f = -12.14$ eV. The dotted line indicates the Fermi energy.

are that the gap between t_{2g} - and e_g -block bands decreases as much as *ca.* 0.3 eV, and the Fermi energy increase slightly. Interactions between FeOCl lattice and Li intercalant may influence the band gap. Charge transfer from Li to the

Table 2. The Net Charge of $(\text{FeOCl})_{16}$ and $(\text{FeOCl-Li}_{1/2})_{16}$

$(\text{FeOCl})_{16}$		$(\text{FeOCl-Li}_{1/2})_{16}$	
Atom	Net charge	Atom	Net charge
Fe	1.7718	Fe	1.3107
O	-1.2109	O	-1.2334
Cl	-0.5609	Cl	-0.4125
		$\text{Li}_{1/2}$	0.3352

The Net charge of each atom is averaged for all atoms in cluster.

Table 3. The Reduced Overlap Population

	FeOCl	FeOCl-Li _{1/2}
Fe-O	0.3291	0.3154
Fe-Cl	0.3900	0.3872

LU-band of FeOCl shifts up the Fermi energy level. When the charge transfer occurs there are 11 electrons to fill the 6 t_{2g} -block band. It is remarkable that the 6th band is partially filled and a little bit dispersive among the t_{2g} -block band. That is, the partially filled band may be responsible for the conductivity increase of FeOCl-Li_{1/2} intercalation complex. The DOS curve, shown in Figure 9, also shows that the lithiation does not influence the electronic structure but causes the upward shift of the Fermi energy level of the host.

Net charges of the constituting atoms were estimated with the Mülliken population analysis. We compare the results obtained from the calculation for 16 mer cluster of FeOCl with its lithium intercalation complex in Table 2. The net charge of Fe decreases from 1.77 to 1.31, whereas that of O atom nearly does not change. Oddly enough one finds that chlorine atom lose its electron as much as 0.15 e^- during the lithiation. These results may suggest that the Fe-Cl bond act as an electron flowing pathway. The partial oxidation of chlorine atom can be understood if we consider the structure of FeOCl-Li_{1/2}. As seen in Figure 7, a lithium atom is located in the octahedral sites consisting of five chlorines and one oxygen atom. Thus the lithium atom drains the electron from the neighboring chlorine atoms.

We perform the reduced overlap population (ROP) analysis for Fe-Cl and Fe-O bond before and after the intercalation. The ROP of a bond is defined as follows:

$$\text{ROP} = 2 \sum_{\alpha} \sum_{i \in A} \sum_{j \in B} n_{\alpha} C_{i\alpha} C_{j\alpha} S_{ij} \quad (3)$$

where n_{α} is the occupation of the α th MO. It has been used successfully as an indication of the strength of a given bond. Table 3 suggests that the Fe-O bond becomes weaker than Fe-Cl bond does due to intercalation. This would be easily rationalized with the COOP curves shown in Figure 5. The bonding nature of Fe-O above the Fermi level is antibonding. Filling the antibonding orbital of Fe-O with transferred electron weaken the Fe-O bond. ROP data are deeply related to the such properties as force constant, vibrational energy, and dissociation energy.¹⁹ Spectroscopic experiments (e.g., far IR, UPS) could verify the obtained result.

Discussion

There have been some efforts to establish a correspondence between the finite cluster model calculation and the band calculation.^{20,21} It is expected that the cluster model approximation converges to the band model as the size of cluster increases. But how large the size of the cluster model is compatible with band model? In the present work, these two types of calculations are plainly consistent with each other in spite of the small cluster size (we use the $2 \times 2 \times 2$ cluster model). It is promising that the calculation with the small cluster gives the result compatible of band calculation.

Since many experimental results claim that FeOCl-Li_x complex decomposes if $x > 0.5$, we have modeled the lithium intercalation complex as FeOCl-Li_{1/2}.²² Since Li can occupy two different sites in the unit cell we must choose one of these two sites. For the ease of computation, we fill only one site of them consistently, so that the translational symmetry is conserved. This choice may have little influence on the computational result.

As mentioned earlier, this work is nearly an initial step to understand the electronic properties of MOCl system. In the present study, we have mentioned little about the differences among many MOCl. Calculations of MOCl with the changing the central atoms will make it possible to understand why the differences arise.

Summary

The present study of FeOCl and its Li intercalation intercalated complex is an attempts to understand the electronic structure and physical properties of MOCl. We deduce the electronic structure of FeOCl and Li intercalation complex. The charge transfer occurs and the transferred electrons are built up exclusively on Fe atom. The partially filled band may be responsible for the conductivity increase. The band structure of FeOCl shows a characteristics of the 2D compound.

Acknowledgement. This work has been supported by the Korea Science and Engineering Foundation, S.N.U. Dae-woo Research Fund, and Ministry of Education.

References

1. J. V. McCanny, *J. Phys. C: Solid State Phys.*, **12**, 3263 (1979).
2. C. Umrigar, D. E. Ellis, D. S. Wang, H. Krakauer, and M. Posternak, *Phys. Rev.*, **B26**, 4935 (1982).
3. G. Y. Guo and W. Y. Liang, *J. Phys. C: Solid State Phys.*, **20**, 4315 (1987).
4. P. Palvadeau, L. Coic, J. Rouxel, and J. Portier, *Mat. Res. Bull.*, **13**, 221 (1978).
5. J. P. Venien, P. Palvadeau, D. Schreich, and J. Rouxel, *Mat. Res. Bull.*, **14**, 891 (1979).
6. J. A. Maguire and J. J. Barewicz, *Mat. Res. Bull.*, **22**, 1217 (1987).
7. H. Schäfer-Stahl and R. Abele, *Angew. Chem. Int. Ed. Engl.*, **19**, 1573 (1984).
8. S. M. Kuzlarich, J. F. Ellena, P. D. Stupik, W. M. Reiff, and B. A. Averill, *J. Am. Chem. Soc.*, **109**, 4561 (1987).
9. S. Kikkawa, F. Kanamaru, and M. Koizumi, *Bull. Chem.*

- Soc. Jpn.*, **52**, 962 (1979).
10. J. Rouxel, P. Palvadeau, J. P. Venien, J. Villieras, P. Janvier, and B. Bujoli, *Mat. Res. Bull.*, **22**, 1217 (1987).
 11. M. H. Whangbo and R. Hoffmann, *J. Am. Chem. Soc.*, **100**, 6093 (1977).
 12. E. Canadell and M. H. Whangbo, *Chem. Rev.*, **91**, 965 (1991).
 13. T. A. Albright, J. K. Burdett, and M. H. Whangbo, "Orbital Interactions in Chemistry", John Wiley & Sons (1985).
 14. M. D. Lind, *Acta Cryst.*, **B26**, 1058 (1970).
 15. R. H. Summerville and R. Hoffmann, *J. Am. Chem. Soc.*, **98**, 7240 (1976).
 16. A. Villesuzanne, J. Hoarau, L. Ducasse, L. Olmedo, and P. Hourquebie, *J. Chem. Phys.*, **96**, 495 (1992).
 17. S. Hwang, Y. H. Jang, and H. Kim, *Bull. Korean Chem. Soc.*, **12**, 635 (1991).
 18. G. Villeneuve and P. Palvadeau, *Mat. Res. Bull.*, **17**, 1407 (1982).
 19. (a) P. Politzer and S. D. Kastan, *J. Phys. Chem.*, **80**, 385 (1976); (b) T. S. Kusma and A. L. Companion, *Surface Sci.*, **195**, 59 (1988).
 20. R. P. Messmer, *Phys. Rev.*, **B15**, 1811 (1975).
 21. G. H. Ryu and H. Kim, *Bull. Korean Chem. Soc.*, **12**, 544 (1991).
 22. Z. Takehara, K. Kanamura, N. Imanishi, and C. Zhen, *Bull. Chem. Soc. Jpn.*, **62**, 3609 (1989).

Solution Dynamics and Crystal Structure of $\text{CpMoOs}_3(\text{CO})_{10}(\mu\text{-H})_2[\mu_3\text{-}\eta^2\text{-C(O)CH}_2\text{Tol}]$

Joon T. Park*, Jeong-Ju Cho*, Kang-Moon Chun†, Sock-Sung Yun†, and Sangsoo Kim‡

*Department of Chemistry, Korea Advanced Institute of Science and Technology, Taejeon 305-701

†Department of Chemistry, Chungnam National University, Taejeon 305-764

‡Lucky Ltd., R & D Center, Taejeon 305-343. Received October 6, 1992

The tetranuclear heterometallic complex $\text{CpMoOs}_3(\text{CO})_{10}(\mu\text{-H})_2[\mu_3\text{-}\eta^2\text{-C(O)CH}_2\text{Tol}]$ (**1**, Cp = $\eta^5\text{-C}_5\text{H}_5$, Tol = *p*-C₆H₄Me) has been examined by variable-temperature ¹³C-NMR spectroscopy and by a full three-dimensional X-ray structural analysis. Complex **1** crystallizes in the orthorhombic space group *Pna*2₁, with *a* = 12.960(1) Å, *b* = 11.255(1) Å, *c* = 38.569(10) Å, *V* = 5626(2) Å³ and $\rho(\text{calcd}) = 2.71 \text{ g cm}^{-3}$ for *Z* = 8 and molecular weight 1146.9. Diffraction data were collected on a CAD4 diffractometer, and the structure was refined to *R_F* = 9.7% and *R_w* = 9.9% for 2530 data (MoK α radiation). There are two essentially equivalent molecules in the crystallographic asymmetric unit. The tetranuclear molecule contains a triangulated rhomboidal arrangement of metal atoms with Os(2) and Mo at the two bridgehead positions. The metal framework is planar; the dihedral angle between Os(1)-Os(2)-Mo and Os(3)-Os(2)-Mo planes is 180°. A triply bridging (μ_3, η^2) acyl ligand lies above the Os(1)-Os(2)-Mo plane; the oxygen atom spans the two bridgehead positions, while the carbon atom spans one bridgehead position and an acute apical position. The molecular architecture is completed by an η^5 -cyclopentadienyl ligand and a semi-triply bridging carbonyl ligand on the molybdenum atom, and nine terminal carbonyl ligands—four on Os(3), three on Os(1), and two on Os(2). The two hydride ligands are inferred to occupy the Os(1)-Os(2) and Mo-Os(3) edges from structural and NMR data.

Introduction

In previous work,¹ we have described that the reaction of $(\mu\text{-H})_2\text{Os}_3(\text{CO})_{10}$ with $\text{Cp}(\text{CO})_2\text{Mo}(\text{CTol})$ (Cp = $\eta^5\text{-C}_5\text{H}_5$, Tol = *p*-C₆H₄Me) has yielded three MoOs₃ mixed-metal clusters including the $\mu_3\text{-}\eta^2$ -acyl compound $\text{CpMoOs}_3(\text{CO})_{11}[\mu_3\text{-}\eta^2\text{-C(O)CH}_2\text{Tol}]$ as the major product. Initial decarbonylation of this complex with Me₃NO/MeCN followed by reaction with dihydrogen has produced the dihydride complex $\text{CpMoOs}_3(\text{CO})_{10}(\mu\text{-H})_2[\mu_3\text{-}\eta^2\text{-C(O)CH}_2\text{Tol}]$ (**1**) in a quantitative yield. Synthesis and spectroscopic characterization of compound **1** has been published.^{1a,c} We herein report full details of solution dynamics and X-ray structural analysis of the dihydrido acyl complex **1**, which has been previously shown to undergo scission of the acyl C-O bond^{1a,c} induced by the hydride ligands.

Experimental Section

General Comments. Carbon-13(¹³C) CO-enriched H₂Os₃(¹³CO)₁₀² and Cp(CO)₂Mo(CTol)³ were prepared as described in the literature. ¹³C-NMR (75 MHz) spectra were recorded on a Bruker AM-300 spectrometer. Cr(acac)₃ (ca 0.02 M) was added to ¹³C samples as a shiftless relaxation reagent.

Preparation of ¹³CO-enriched **1***. Carbon-13 CO-enriched $\text{CpMoOs}_3(^{13}\text{CO})_{11}[\mu_3\text{-}\eta^2\text{-C(O)-CH}_2\text{Tol}]$ was prepared from the reaction of ¹³CO-enriched H₂Os₃(¹³CO)₁₀ (ca 50% enrichment) with Cp(CO)₂Mo(CTol) and then this complex was utilized to prepare $\text{CpMoOs}_3(^{13}\text{CO})_{10}(\mu\text{-H})_2[\mu_3\text{-}\eta^2\text{-C(O)CH}_2\text{Tol}]$ (**1***) by the reported procedures.^{1c}

X-ray Data Collection and Structure Solution of **1.** Crystals were grown by slow recrystallization from a mixture of dichloromethane-petroleum ether at room temper-